Preparation of a BiTeI polar semiconductor with a strong asymmetric inversion

Andrzej Materna[1]

The paper describes the synthesis and crystallization processes of a BiTeI polar semiconductor, carried out by a modified vertical Bridgman method (VB), or/and by CVT (chemical vapor transport) method, in a horizontal position. For BiTeI samples, the measurements were performed by Van der Pauw method and by the structural techniques (EDS, XRD and Raman spectroscopy), which confirmed the presence of a pure BiTeI phase in the obtained materials.

Key words: topological insulator, BiTeX (X = I, Br, Cl) compounds, VB method, CVT method

Otrzymywanie polarnego półprzewodnika BiTeI, wykazującego silną asymetrię inwersji

W pracy opisano procesy syntezy i krystalizacji polarnego półprzewodnika BiTeI metodą transportu chemicznego (CVT) w układzie poziomym oraz zmodyfikowaną, pionową metodą Bridgmana (VB). Dla przygotowanej serii próbek, wykonano pomiary własności transportowych (metodą Van der Pauwa), które wykazały dużą ruchliwość nośników, w temperaturze 77K. Badania strukturalne wykonane za pomocą technik mikroanalizy rentgenowskiej EDS (energy dispersive spectroscopy), rentgenowskiej analizy dyfrakcyjnej XRD (X-ray diffraction analysis) oraz spektroskopii Ramana, potwierdziły obecność czystej fazy BiTeI w otrzymanych materiałach.

Słowa kluczowe: izolator topologiczny, związki BiTeX (X = I, Br, Cl), krystalizacja metodą VB, krystalizacja metodą CVT

1. Introduction

The subject area related to the existence of topological insulators dates back to 2008 [1]. In condensed matter physics, the appearance of a topologically protected state on the surface of a 3D topological insulator and the related phenomena originate from the presence of a strong Spin--Orbit Interaction (SOI) and Time Reversal Symmetry (TRS). This class of insulators is represented by symmetrical compounds, such as: Bi_2Se_3, Bi_2Te_3, Sb_2Te_3 [2]. The great value of spin-orbit coupling can lead not only to the formation of the phases of a topological insulator or to unconventional superconductivity [3 - 4], but also to other quantum effects.

One of the aforementioned phenomena referes to electron spin polarization in the absence of an applied external magnetic field, known as the *Rashba effect*. The Rashba effect splitting a momentum-dependent spin bands in 2D condensed matter systems (heterostructures and surface states), is similar to the splitting of particles and anti-particles in the Dirac Hamiltonian [1].

The Rashba effect results in the removal of degeneracy and splitting of the oppositely spin-polarized states of electrons (spin-split) [5]. This mechanism is schematically shown in Fig. 1 in a diagram of the band structure for the BiTeI material in its conduction band [3].

The possibility to observe such unique quantum effects within a single system makes the materials with a great value of spin-orbit coupling promising for their use in spintronics. The name Spintronics (spin electronics) is used to stress that it refers to the electron spin and not the electron charge. The key requirement is the ability to change the spin not in the magnetic but in the electric

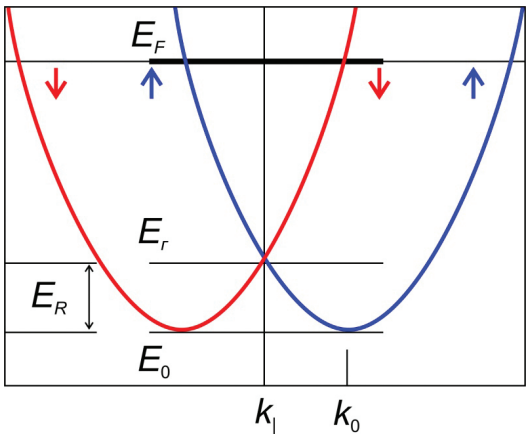

Fig. 1. Band structure diagram of BiTeI, with a visible spin splitting (displacement) *Rashba effect* - in the conduction band. E_F - Fermi level, E_R - Rashba energy, $E_0 = E_\Gamma$ - size of the energy gap. Colors indicate the opposite polarity of spins (spin-up, spin-down) [3].

Rys. 1. Schemat struktury pasmowej w BiTeI, z widocznym rozszczepieniem (przesunięciem) spinu *efekt Rashby*, w paśmie przewodnictwa. E_F - poziom energii Fermiego, E_R - energia Rashby, $E_0 = E_\Gamma$ - wielkość przerwy energetycznej. Kolorami oznaczono spiny o przeciwnej polaryzacji [3].

[1] *Institute of Electronic Materials Technology*, 133 Wólczyńska Str., 01-919 Warsaw, Poland, e-mail: Andrzej.Materna@itme.edu.pl

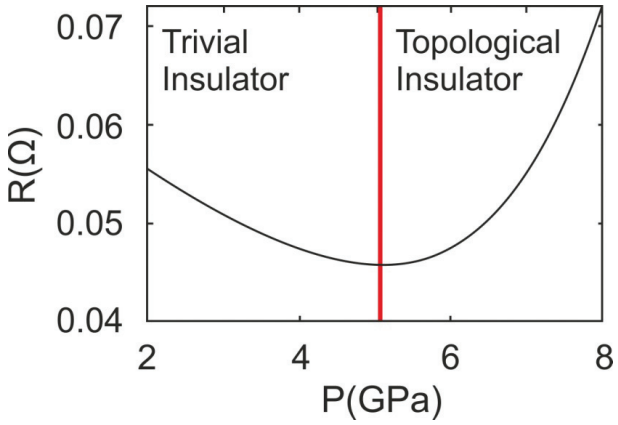

Fig. 2. Resistance - *R* (Ω) of BiTeI semiconductor, as a function of pressure *P* (GPa). At the level of ca. 5 GPa, the boundary (red line) of the phase transition from a trivial insulator state (polar semiconductor) to a topological insulator state becomes visible [11].

Rys. 2. Oporność - *R* (Ω) półprzewodnika BiTeI, w funkcji ciśnienia *P* (GPa). Na poziomie ok. 5 GPa, widoczna jest granica (czerwona linia), przejścia fazowego ze stanu izolatora trywialnego (polarnego półprzewodnika) do stanu izolatora topologicznego [11].

field. During the flow of a spin-polarized current, both the electric charges and the spins are being transferred, i.e. it is a flow of carriers (electrons or holes) with a specific spin. One of the goals of spintronics is to control the electron spin and as such it was applied in *spin-field* devices and in spin Hall effect transistors. [6 - 8]. The operation of spintronic devices utilizes the interaction between spin magnetic moment of the electron and the effective magnetic field. This interaction is of a relativistic nature and results from relativistic quantum mechanics, based on Dirac equations [9].

The crystalline compounds described above are represented by a BiTeI polar semiconductor, belonging to a new class of bismuth-tellurium ternary halides of the formula BiTeX (X = I, Br, Cl). These compounds are characterized by an asymmetric, inverted structure and by one of the greatest values of the Rashba coefficient, which amounts to αR ~3.8 eVÅ, while for other materials this coefficient is of the order of αR ~ (0.1 - 0.3) eVÅ, [5]. Therefore, BiTeI can be used as a primary material in fast switching systems, quantum computers and - in the near future- it may provide a basis for the development of a new field of physics, namely *semiconductor spintronics* [6]. Additionally, the phase transitions are possible in the BiTeI system, making it the only material, where the transition from a topologically trivial state (semiconducting state) to a topological insulator state and then to a topological superconducting state can be tested [4, 7].

Under atmospheric pressure conditions, BiTeI is a polar semiconductor (a trivial insulator), in which large Rashba splitting and energy gap can be observed. The calculated energy gap for the BiTeI system, based on the density functional theory (DFT), is $E_\Gamma \sim 0.8$ eV. When ignoring the spin-orbit interaction (SOI) [10], this value is almost twice as high as that obtained experimentally. Under the influence of the applied external pressure of the order of several GPa, this semiconductor undergoes the band inversion and a transition to a topological insulator state (Fig. 2) [11], making the BiTeI compound one of the first examples of the realization of a topological phase transition. Such a pressure-induced topology transformation in the structure of BiTeI is reversible [12]. Moreover, at higher pressures exceeding 10 GPa, the appearance of a topological superconducting state becomes possible [5].

The occurrence of the aforementioned transition is related to the quality of the crystal. As it is well known the low resistance of this material results from the presence of various defects [11]. Therefore, it becomes extremely important to find a method for the production of BiTeI crystals with a very high resistance. The first step to obtain such crystals is the synthesis of high purity components.

The synthesis of the BiTeI compound has proceeded according to the overall chemical equation:

$$Bi_2Te_3 + BiI_3 \rightarrow 3BiTeI,$$

where: Bi_2Te_3 - is a symmetrical topological insulator, BiI_3 - bismuth halide (iodide) - (Fig. 3).

A detailed description of the synthesis process is given in Section 2.1.

The structures of compounds: Bi_2Te_3 and BiTeI are schematically presented below. Fig. 3a shows a part of a layered structure of a hexagonal crystal lattice of a symmetrical topological insulator Bi_2Te_3, with a five-layer (quintuple) symmetrical unit cell. On the other hand,

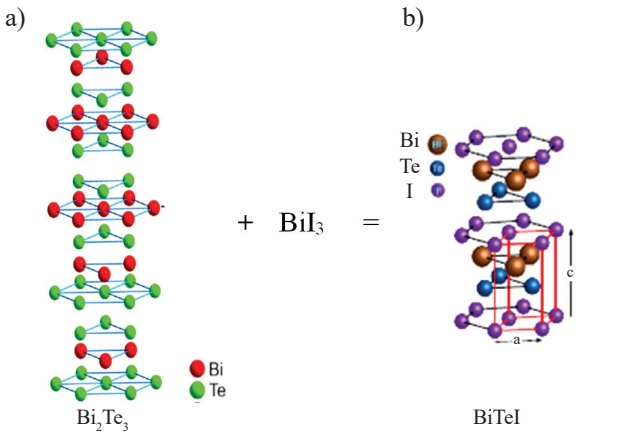

Fig. 3. The BiTeI compound structure, a) symmetrical unit cell (quintuple layers) of a Bi_2Te_3 topological insulator, b) asymmetrical unit cell with inversion of a BiTeI insulator with the dimensions indicated. Lattice parameters of BiTeI compound in the hexagonal plane a, along the growth axis – c are: a = 4.34 Å and c = 6.854 Å (according to Ishizaka *et al.*[5]).

Rys. 3. Struktura związku BiTeI, a) Symetryczna, pięciowarstwowa (kwintetowa) komórka izolatora topologicznego Bi_2Te_3, b) Asymetryczna z inwersją - komórka elementarna związku BiTeI, z widocznymi rozmiarami. Parametry sieci krystalicznej BiTeI w płaszczyźnie sześciokątnej - a, wzdłuż osi wzrostu - c, wynoszą: a = 4,34 Å i c = 6,854 Å (wg Ishizaka *et al.*[5]).

Fig. 3b shows the unit cell of a synthesized asymmetrical BiTeI semiconductor, which is also characterized by a hexagonal crystal lattice. In the three-layer (triple), asymmetrical unit cell of BiTeI, we can see the inversion of atomic layers arranged in the following order along the vertical direction of the c axis: I-Bi-Te-I-Bi-Te-I ...

The key component in the BiTeI lattice (in Fig. 3b) is bismuth (Bi), a heavy element whose atom exhibits a strong SOI. Its triangular layer is asymmetrically arranged between tellurium (Te) and halogen (I or Br, or Cl) layers. A layer of Bi, together with a layer of Te, i.e. an element of a similar lattice geometry to that of metallic bismuth, form a positively charged layer (BiTe)+. The zones of Van der Waals interactions occur between the layers of tellurium (Te) and iodine (I).

The concentration of *n-type* carriers in this material, obtained by Ishizaka *et al.* [5], was as high as $n_{bulk} \sim 4.5 \cdot 10^{19}$ cm^{-3}. According to Tournier-Colletta *et al.* [13], the lattice parameters for the BiTeI semiconductor are: a = 4.341 Å and c = 6.852 Å. However, the lattice, parameters of BiTeI, calculated by Shiyi Zhou *et al.* [10], are a = 4.32834 Å, c = 6.90572 Å. The authors assumed their data to be in agreement with the experimental results, i.e. a = 4.3392 Å, c = 6.854 Å, because of a small deviation from the measured values, i.e. not exceeding 1.5%.

2. Experimental - preparation and examination of BiTeI semiconductor

2.1. Synthesis of BiTeI compound

The phase diagram of the ternary compound Bi-Te-I (Fig. 4a) shows that the synthesis reaction can also result in other products formed under similar conditions, but of different chemical formulas, reflecting their different compositions, e.g.: C_1 - BiTeI, C_2- Bi_4TeI, C_3 - $Bi_4TeI_{1.25}$.

In order to determine the temperature for the synthesis process of the BiTeI compound, we used a pseudo-binary system BiI-Te (Fig. 4b). However, for the *laboratory* synthesis of the BiTeI insulator, we considered a phase diagram of the pseudo-binary, in which the components (reactants) for the synthesis were: BiI_3 and bismuth telluride - Bi_2Te_3.

The synthesis of the BiTeI compound proceeded in the etched and evacuated quartz ampoules, where the weighted samples of two compounds were placed: BiI_3 and a topological insulator - Bi_2Te_3 (according to Fig. 3).

Bismuth iodide - BiI_3 with a purity of ca. 99.5% is hygroscopic, quickly undergoes oxidation, and most of all, it is very toxic. For this reason, it was loaded in anaerobic chambers, in the atmosphere of a dry inert gas (f.e. Ar). The second reactant, i.e. bismuth telluride - Bi_2Te_3, as a raw material of high purity (at least 5N), was prepared earlier in a separate process, before the proper synthesis of BiTeI. Then, the loaded quartz reaction ampule of

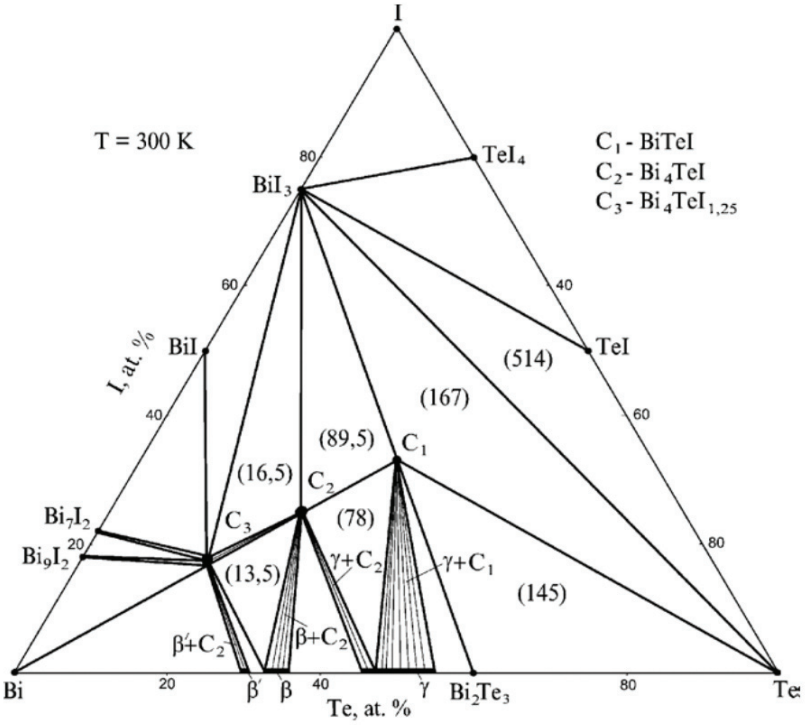

Fig. 4a. Phase diagram in the isothermal section (300 K) for Bi-Te-I [14].
Rys. 4a. Diagram fazowy w układzie izotermicznym dla: Bi-Te-I (300 K) [14].

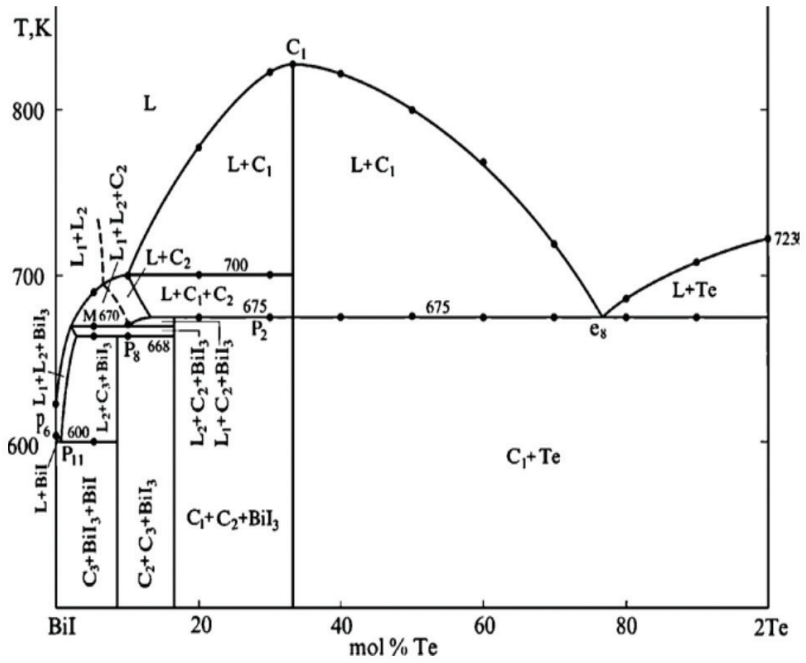

Fig. 4b. Phase diagram in the pseudobinary BiI-Te system [14].
Rys. 4b. Diagram fazowy w pseudo-binarnym układzie BiI-Te [14].

a diameter of 24 mm was placed in a three-zone resistance furnace. The homogeneous thermal field was characterized by an axial temperature gradient of ranging 2 - 3°C/cm and the maximum temperature did not exceed 640°C. The synthesis process took ~ 30 hours.

2.2. Crystallization of BiTeI

BiTeI semiconductor crystals can be obtained by several methods of crystallization, e.g. CVT, VB, HB, etc. This article focuses on CVT and VB methods.

1. The horizontal CVT (*Chemical Vapor Transport*) method in I_2 vapor is a two-step process. In the first stage, components BiI_3 and Bi_2Te_3 undergo a stoichiometric synthesis. After BiTeI crystallization, the ampoule content is unloaded. In the second stage, the quartz ampoules are loaded with a weighted samples of the prepared BiTeI precursor by placing it in the source zone of the ampoule, together with a weighted sample of iodine. The sublimating iodine serves for a transport agent of the particles from the source zone (at higher temperature) to the deposition zone (at lower temperature). When the vacuum reached the level of p ~ 4 x 10^{-6} Tr, the ampoule was sealed and placed in a horizontal furnace for the deposition of layers by the CVT method - see a diagram in Fig. 5. Due to a rapid evaporation of iodine vapors, iodine (I_2) loading took place under special conditions, with the use of a refrigerant.

2. The vertical VB (*Vertical Bridgman*) method is a one-step process. The synthesis and crystallization processes take place in one quartz ampoule, which is loaded with stoichiometric weighted samples of BiI_3, together with the previously prepared Bi_2Te_3. Then, after the vacuum reaches the level of p ~ 4 x 10^{-6} Tr, the ampoule was sealed and positioned in the upper zone of a vertical furnace for the crystallization of BiTeI.

The letter C denotes the material obtained by CVT method, e.g. BTI-C2.

During the first stage of the work, the measurements of temperature distribution in the horizontal furnace (Fig. 5) were carried out, in the temperature range 350 - 500°C, and in the vertical furnace, in the temperature range 250 - 600°C. The measurements of other technological parameters were also performed, namely:

a) axial temperature gradients in the source and deposition zones in the horizontal furnace; the time of BiTeI deposition process was selected on the basis of the precursor decomposition time - in the CVT method.

b) vertical and radial temperature gradients along the axis in the vertical furnace and the crystallization rate - v_k in the assumed thermal conditions - in the VB method.

In the second stage, the processes of the synthesis and deposition of the layers of BiTeI were carried out by the CVT method. The synthesis and crystallization of BiTeI were carried out by the VB method, according to the assumed parameters.

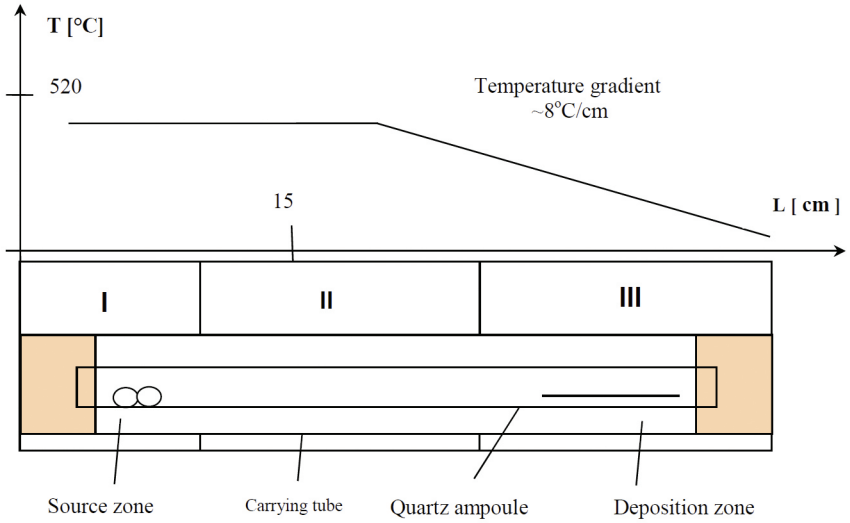

Fig. 5. Schematic temperature distribution in a three-zone (I, I, III) horizontal furnace in the temperature range 500 - 350°C, in the source and deposition zones, respectively, for the crystallization of BiTeI by CVT (Chemical Vapor Transport) method in I_2 vapor.
Rys. 5. Schematyczny rozkład temperatury w piecu poziomym, trójstrefowym (I, II, III), w zakresie temperatur: 500 - 350°C, odpowiednio w strefie źródłowej (z prekursorem) i w strefie osadzania, dla krystalizacji związku BiTeI metodą CVT, w parach I_2.

2.2.1 Crystallization of BiTeI compound by CVT method

After a preliminary synthesis of the BiTeI precursor, loading the reactants and the evacuation of the air from the reaction ampoule, the ampoule was placed in a horizontal furnace (Fig. 5) and the process of BTI-C1 deposition was performed by the CVT method. The total deposition time took ca. 150 hours.

As a result of the BTI-C1 process, a small monocrystaline plate (Fig. 6) of the following dimensions: 6 × 8 × 0.1 mm^3, precipitated on the inner wall of the ampoule, in the middle of its length.

After the composition determination by the XRD method, it was found that the lines of the visible peaks did not overlap with those indicated for the standard of a BiTeI material. The obtained phase was Bi_2Te_3, which became separated from the BiTeI precursor and crystallized as a single crystal wafer in a horizontal system. The measurement carried out in the plane of the wafer, showed hkl (001 lines), characteristic of Bi_2Te_3, indicating (001) orientation on the wafer - Fig. 7.

The possible cause of this phenomenon was the evaporation of some part of the mass of iodine - I_2, assumed as the particle transporting agent, while obtaining the vacuum in the reaction ampoule and the decomposition of the BiTeI precursor.

In the next BiTeI crystallization process, the mass of iodine was increased, the pumping time was shortened by a half, the final vacuum level was reduced to 2 x 10^{-5} Tr, the deposition time was increased and the mass of the BiTeI precursor was left at the same level. Then the growth of the BTI C2 was carried out.

As a result of the BTI C2 process, two parts of the deposited BiTeI insulator layers were obtained in the initial and terminal parts of the reaction ampoule - (Fig. 8a).

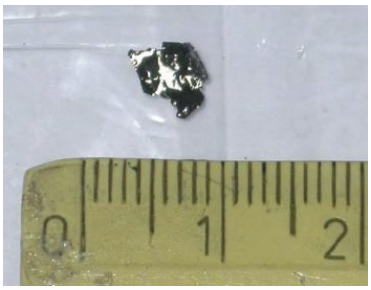

Fig. 6. A layer deposited in the BTI C1 process, as a single crystal wafer - Bi_2Te_3.
Rys. 6. Osadzona warstwa, w procesie BTI C1, w postaci monokrystalicznej płytki Bi_2Te_3,

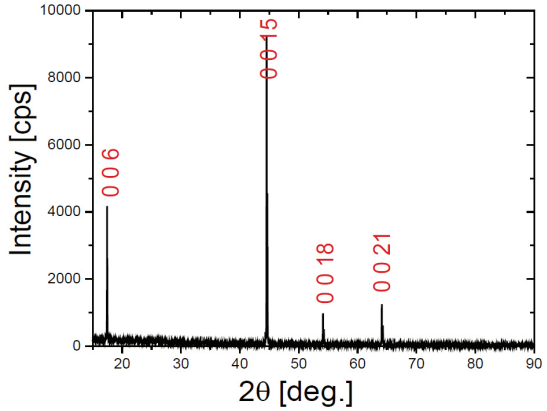

Fig. 7. Diffraction pattern (XRD) of a sample from BTI C1 process; visible single crystal cleavage plane of (001) crystallographic orientation. The indicated indexes of the observed reflections correspond to a Bi_2Te_3 phase (SG R-3m).
Rys. 7. Dyfraktogram XRD próbki z procesu BTI-C1; widoczna monokrystaliczna płaszczyzna łupliwości o orientacji (001). Oznaczone indeksy obserwowanych refleksów dyfrakcyjnych, odpowiadają fazie Bi_2Te_3 - (SG R-3m).

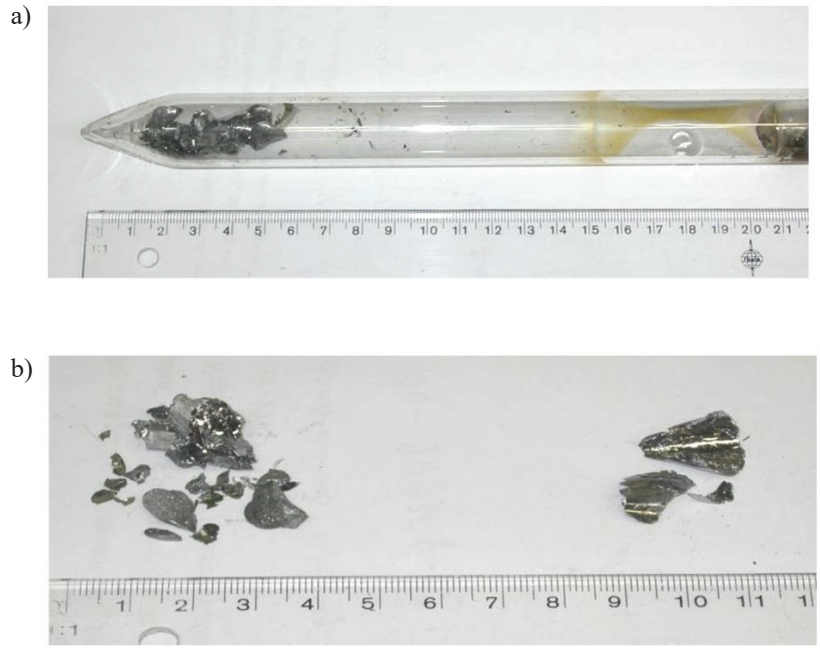

Fig. 8. Preparation of BiTeI semiconductor in BTI C2 process by CVT method in a horizontal configuration: a) view of the reaction ampoule, b) the reactants of the precursor (left side) and the deposited BiTeI layers (right side).
Rys. 8. Proces BTI C2 metodą CVT w układzie poziomym, półprzewodnika BiTeI; a) widok ampuły reakcyjnej), b) substraty prekursora (po lewej) i osadzone warstwy BiTeI (po prawej stronie).

Fig. 8a shows the horizontal view of the ampoule after the BTI-C2 semiconductor growth by the CVT method. In its initial, conical part we can see the disintegrated pieces of the BiTeI precursor and the layer deposited on the walls of the ampoule in the source temperature zone. In its opposite part (right end), we can observe the second portion of the deposited layer (in the deposition zone) and a yellowish precipitate after the crystallization of iodine vapor. Fig. 8b shows the view after unloading the reaction ampoule and the separation of the pieces of the synthesized precursor, i.e. the BiTeI compound (left side) from the deposited BiTeI layers (right side). The visible conical shape of the latter sample results from the internal shape of the conical part of the ampoule, on which the layer was deposited. The entire size of the deposited layer was around 25 × 15 mm^2 and its thickness was around 0.2 - 0.4 mm^2. The total time of the layer deposition process took around 350 hours. The crystal lattice parameters in the hexagonal plane -a and along the growth axis -c, were determined during the XRD phase analysis of this layer and are discussed below.

Fig. 9 presents the result of the phase composition analysis, performed by the XRD method for the layers obtained from a BTI-C2 process. We can see the reflections characteristic of a BiTeI material.

Fig. 10 shows the result of a Raman spectroscopic examination of the composition of the layers obtained from a BTI-C2 process. These data are similar to those reported by M. K. Tran et al. [9].

After the examination of the phase composition using both methods, it was found that the obtained layers formed

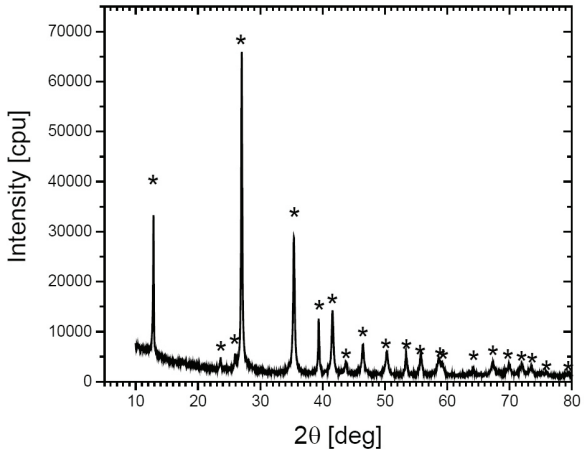

Fig. 9. Diffraction pattern (XRD) of a powdered layer obtained in BTI-C2process. The diffraction reflections corresponding to a pure BiTeI phase are indicateed by the symbol * (SG P3).
Rys. 9. Dyfraktogram sproszkowanej warstwy z procesu BTI-C2. Symbolem * oznaczono refleksy dyfrakcyjne odpowiadające czystej fazie BiTeI (SG P3).

a pure phase of the BiTeI semiconductor, without any precipitates of foreign phases.

2.2.2 Crystallization of BiTeI compound by VB method

As mentioned before, the vertical crystallization of the BiTeI semiconductor was performed using the VB method. The reaction ampoule with a diameter d = 22 mm,

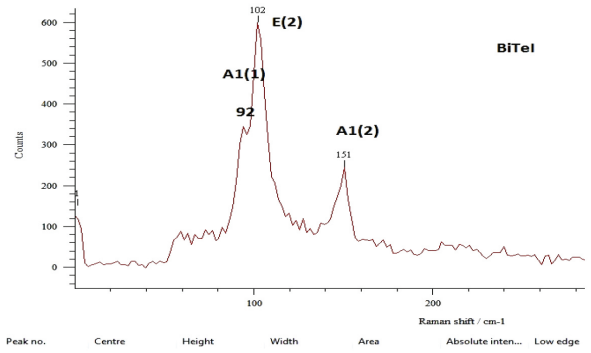

Fig. 10. Raman spectrum for a BTI-C2 sample, with the characteristic energies of modes of A1(1), A1(2) and E(2) symmetry for a pure BiTeI phase.
Rys. 10. Widmo Ramanowskie próbki BTI-C2 z charakterystycznymi dla czystej fazy BiTeI, energiami modów o symetriach A1(1), A1(2) i E(2).

previously loaded with the weighed reactants (BiI_3 and Bi_2Te_3) was exhausted (~ 4 x 10^{-6} Tr), sealed and placed in a vertical furnace. The maximum temperature of the melt was ca. 590°C, the axial temperature gradient was at the level of G_o ~ 26 °C/cm and the crystallization rate was: v_k ~ 4 mm/h. The total time of the crystallization process, together with the preparation was ca. 40 hours.

The BTI-1 crystal obtained in the crystallization process was characterized by the mass of ~ 35 g, diameter 18 mm and length 21 mm. Next, after cutting it perpendicularly to the growth axis (Fig. 11b), four wafers of the size 5 x 5 mm were sampled and subjected to exfoliation with a pressure-sensitive adhesive tape in order to remove a damaged layer. Then the samples went through the structural analyses by a scanning microscope (SEM and EDS) - Figs. 12 - 14.

In order to verify the quality of the obtained material, 12 points were chosen on the surface of the BTI-1/5 sample

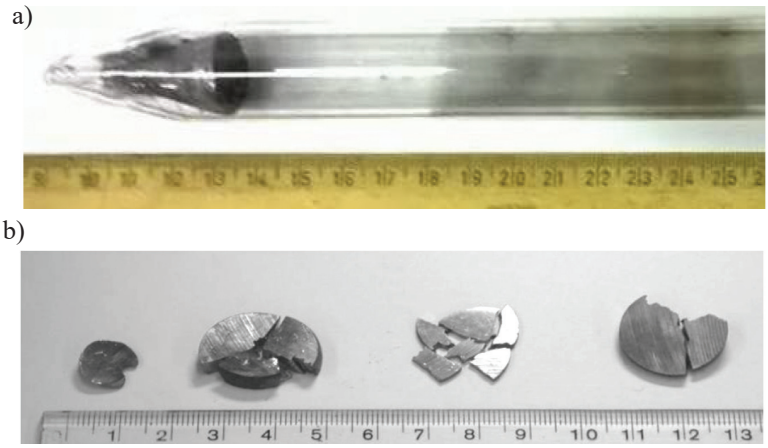

Fig. 11. a) View of the reaction ampoule after BTI-1 crystallization process; b) View of a BTI-1 crystal, after cutting it into the samples of various thickness (approx. 5 mm, 3 mm and 2 mm). The samples were destined for the structural, spectral and electrical measurements. Skew grains are visible on the wafers.
Rys. 11. a) Widok ampuły reakcyjnej z wsadem, po procesie krystalizacji BTI-1; b) Widok kryształu BTI-1 po przecięciu na różne grubości próbek (ok. 5 mm, 3 mm i 2 mm). Próbki przeznaczono na pomiary strukturalne, spektralne i elektryczne. Widoczne skośne ziarna na płytkach.

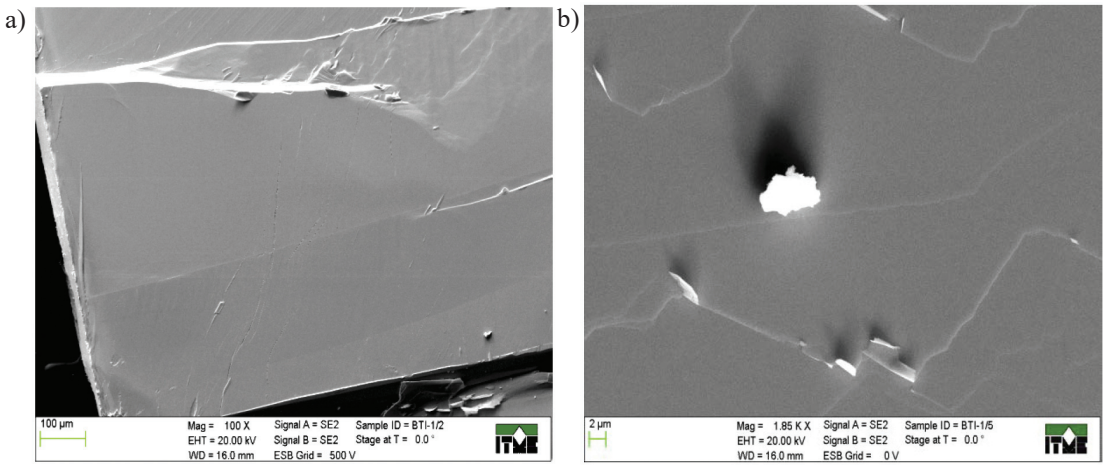

Fig. 12. SEM images of the wafers after exfoliation; visible large, homogeneous surfaces of BTI-1 wafers: a) BTI-1/2 with dimensions of approx. 900 x 600 µm^2, scale bar 100 µm. b) BTI-1/5 with the visible small parts (size 2 - 5 µm) from the previous exfoliation, scale bar 2 µm.
Rys. 12. Obrazy SEM płytek po eksfoliacji, widoczna duże jednorodne, powierzchnie płytek (ziaren) BTI-1. a) BTI-1/2 o wymiarach ok. 900 x 600 µm^2, znacznik 100 µm. b) BTI-1/5 widoczne małe naderwane fragmenty (kawałki) o wymiarach 2 - 5 µm z poprzedniej eksfoliacji. Znacznik 2 µm.

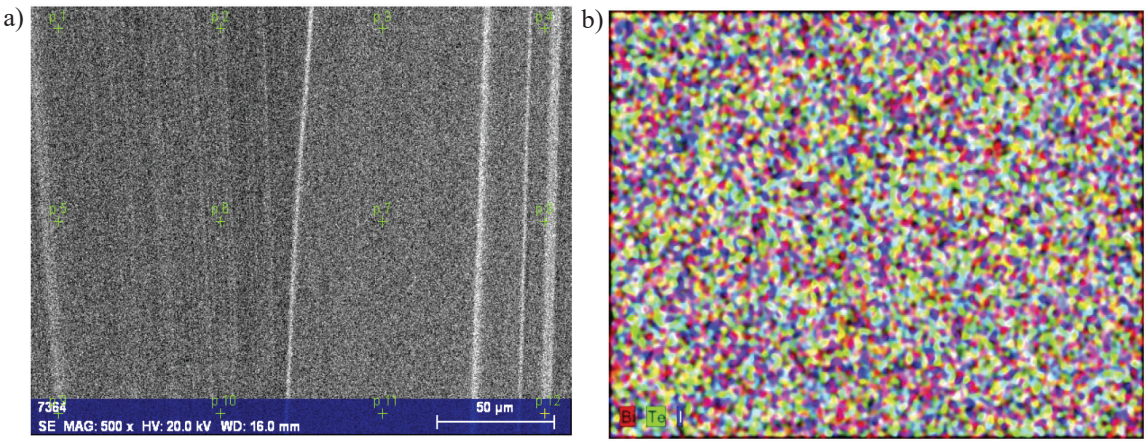

Fig. 13. a) SEM image of a BTI-1/5 wafer (dimensions of approx. 250 x 150 µm), with 12 measuring p 1 - p 12 points (green) for Tab. 1. b) EDS measurement showing a homogeneous, uniform distribution of the elements: Bi-red, Te- green and I -blue.
Rys. 13. a) Obraz SEM płytki BTI-1/5 o wymiarach ok. 250 x 150 µm. z 12 punktami pomiarowymi p 1 - p 12 (zielonymi), do Tab. 1. b) Pomiar EDS. Widoczny równomierny, jednorodny rozkład pierwiastków. Oznaczenia kolorów: Bi-czerwony, Te-zielony, I -niebieski.

Spectrum: p 3

El	AN	Series	unn. C [wt.%]	norm. C [wt.%]	Atom. C [at.%]	Error (1 Sigma) [wt.%]
C	6	K-series	0.00	0.00	0.00	0.00
Al	13	K-series	0.00	0.00	0.00	0.00
Te	52	L-series	26.68	28.81	34.56	0.79
I	53	L-series	25.98	28.05	33.84	0.76
Bi	83	L-series	39.96	43.14	31.60	1.28
		Total:	92.62	100.00	100.00	

Fig. 14. Local elemental analysis of a BTI-1/5 sample by EDS – data for spectrum p 3, Tab. 1.
Rys. 14. Analiza pierwiastkowa EDS dla próbki BTI-1/5, w punkcie – spectrum p 3, Tab. 1.

Tab. 1. Measurement of atomic composition of the elements: Te, I, Bi and the mean value (Te-34.79%, I -33.95%, Bi-31.26%) from 12 points (p 1 - p 12, green crosses - Fig. 13a), located on the wafer surface. The measurement error (sigma), ranges from 0.33 to 0.6%. The theoretical (ideal) distribution is 33.33% for each analyzed element.
Tab. 1. Pomiar składu atomowego pierwiastków: Te, I, Bi oraz uśredniony wynik (Mean value Te 34,79%, I 33,95%, Bi-31,26%) z dwunastu punktów p 1 - p 12 (zielone krzyżyki - Rys. 13a), położonych na powierzchni tej płytki. Błąd pomiarowy (Sigma) waha się od 0,33 do 0,6 %. Teoretyczny (idealny) rozkład wynosi 33,33(3)% dla każdego analizowanego pierwiastka.

Measuring point	Atomic percent (%)		
Spectrum	**Te**	**I**	**Bi**
p1	35.44	34.20	30.36
p2	35.08	34.46	30.47
p3	34.56	33.83	31.60
p4	34.96	33.74	31.30
p5	34.75	33.79	31.46
p6	34.86	33.94	31.20
p7	35.28	34.15	30.56
p8	34.63	34.02	31.35
p9	34.42	33.49	32.09
p10	34.39	34.36	31.25
p11	34.22	33.37	32.40
p12	34.62	34.09	31.29
Mean value:	34.79	33.95	31.26
Sigma:	0.36	0.33	0.60
Sigma mean:	0.11	0.10	0.17

for the measurements of the atomic composition homogeneity. The elements: Te, I and Bi were analyzed at the selected places - Fig. 13a. The results of the composition measurements are presented in Tab. 1.

Figures 15 and 16 show the results of the phase composition tests performed by Raman spectroscopy and XRD methods for the wafers of a size 5 × 5 mm^2, obtained in the BTI-1 process, after the exfoliation.

The XRD measurements were made in a Bragg-Brentano geometry (θ/2θ) - Figs. 7, 9 and 16, using a Rigaku SmartLab 3 kW diffractometer. The *Kα* radiation line of a Cu lamp was used, with the operating parameters: U = 40 kV and I = 30 mA. A Dtex linear detector was applied. The phase analysis and Rietveld analysis of the lattice parameter refinement was carried out using the PDXL program, associated with the ICDD PDF4+2015 crystallographic database.

The samples obtained in VB (BTI 1/2) and CVT (BTI C2) processes consist of a single BiTeI phase of a P3 trigonal structure (the standard number: ICDD 00-043-0650) and are characterized by the following lattice parameters (in the hexagonal notation):

BiTeI standard from ITME crystallographic database
a = 4.3394 Å c = 6.8626 Å

Layers obtained by CVT (BTI C2)
a = 4.3411 Å c = 6.8617 Å

Crystal obtained by VB (BTI 1/2)
a = 4.3412 Å c = 6.8587 Å

The lattice parameters of the layers and crystals obtained in ITME are: a = 4.3411 Å, c = 6.8617 Å and a = 4.3412 Å, c = 6.8587 Å, respectively. These values are consistent with the data reported by the authors from other research laboratories in the world [5,10,13].

In order to improve structural quality and increase the grain size, the next growth process of a BTI-2 semiconductor was carried out using the VB method, reducing the charge mass, the crystallization rate to v_k = 2.5 mm/h, and simultaneously increasing the axial temperature gradient to the level of G_o ~ 35°C/cm.

A BTI-2 crystal that was obtained as a result of the aforementioned process, had the mass of ~ 18 g, diameter 12 mm and length 16 mm, and the grain size ranging from 2 to 7 mm. Then, after cutting it perpendicularly to the axis of the growth (Fig. 17), the wafers with the dimensions of 5 × 5 mm^2 were taken for the electrical tests.

As shown in Fig. 17, the wafers obtained in the BTI-2 process have larger grains than those obtained in the BTI-1 process.

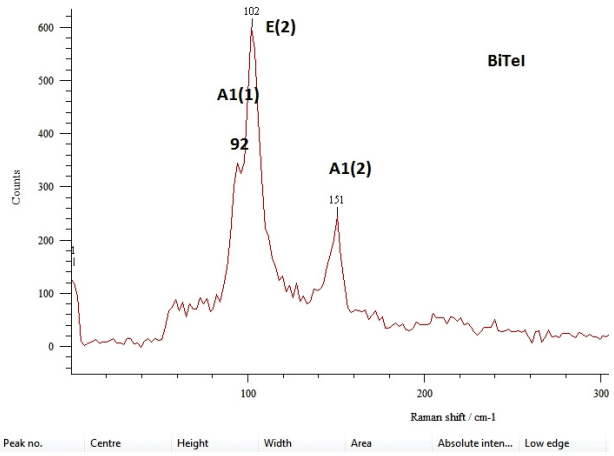

Fig. 15. Raman spectrum of a sample BTI- 1/4, with characteristic energies of modes for the phase of BiTeI (a pure phase without precipitates is visible).
Rys. 15. Widmo Ramanowskie próbki BTI- 1/4 z charakterystycznymi energiami modów dla fazy BiTeI, (widoczna czysta faza, bez wytrąceń).

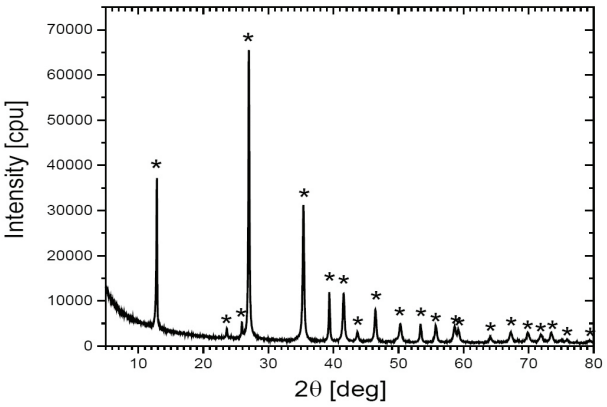

Fig. 16. Diffraction pattern (XRD) of a powdered layer of a BTI-1/2 crystal. A single phase of a BiTeI insulator is visible. Symbol * indicates diffraction reflections corresponding to the BiTeI phase (SG P3).
Rys. 16. Dyfraktogram XRD sproszkowanego kryształu BTI-1/2 widoczna pojedyncza faza izolatora BiTeI. Symbolem* oznaczono refleksy dyfrakcyjne odpowiadające fazie BiTeI (SG P3)

Fig. 17. BTI-2 crystal after cutting it into wafers of a thickness of approx. 4 mm, destined for the structural and electrical measurements.
Rys. 17. Kryształ BTI-2, po przecięciu na płytki o grubości ok. 4 mm. przeznaczone na pomiary strukturalne i elektryczne.

3. Measurements of electrical parameters of a polar semiconductor - BiTeI

Wafers measuring 5 x 5 mm^2 and the thikness $g = 0.4$ mm were prepared for the tests of the electrical properties of a BiTeI semiconductor by the Van der Pauw method. The results for the wafers originating from both crystallization methods (VB and CVT) are presented in Tab. 2. As an example, a photo of the samples obtained from the BTI-2 process and with the contacts soldered, is shown in Fig. 18. The measurements were carried out at temperature 295 K (RT) and 77 K.

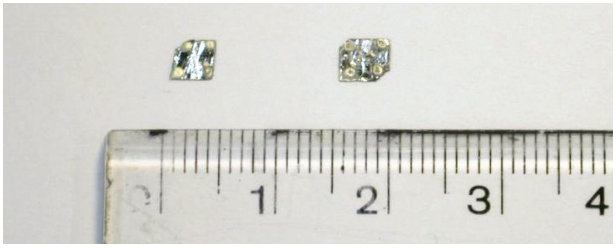

Fig. 18. The samples with the dimensions 5 × 5 mm, after exfoliation from the crystals: BTI-2/1 (left) and BTI-2/2 (right), with the soldered contacts (Ag), destined for electrical measurements by the Van der Pauw method.
Rys. 18. Eksfoliowane próbki o wymiarach 5 × 5 mm. z kryształu BTI-2/1 (lewa) i BTI-2/2 (prawa), z przylutowanymi kontaktami (Ag), przeznaczone do pomiarów elektrycznych metodą Van der Pauwa.

In accordance with the results obtained in transport measurements by the Van der Pauw method at room temperature (RT), presented in Tab. 2, in a layer originating from the BTI-C2 process and prepared by CVT, the carriers concentration of n-type was ca. twice lower than their concentration in the samples of the crystals obtained by the Bridgman vertical method (VB).The carriers mobility in the same sample (BTI-C2), was ca. twice as low in comparison with the mobility in a material obtained by the VB method. It could indicate a better structural quality and a greater purity of the samples of BiTeI crystals originating from VB processes.

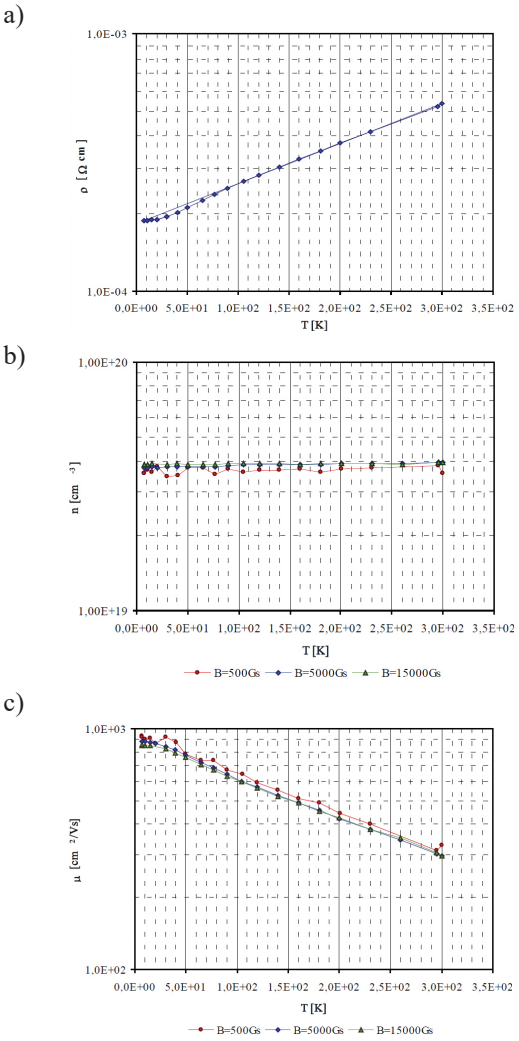

Fig. 19. Results of measurements of the electrical parameters for samples from the BTI-2/2 wafer: a) the resistivity $\rho = f(T)$, b) the carrier concentration $n = f(T)$, c) the mobility $\mu = f(T)$, as a function of temperature. N-type conduction exhibits a stable value over the whole measured temperature range.
Rys. 19. Wyniki pomiarów parametrów elektrycznych próbek z płytki BTI-2/2 w funkcji temperatury: a) oporności właściwej $\rho = f(T)$, b) koncentracji nośników $n = f(T)$, c) ruchliwości $\mu = f(T)$. Typ przewodnictwa n, wykazuje stabilną wartość w całym zakresie mierzonych temperatur.

Tab. 2. Measurements of the electrical parameters: carrier concentration n, mobility μ and resistivity ρ, for BiTeI semiconductor samples, obtained using the VB and CVT methods. Measurement temperature was 295 K (RT) or 77 K. All the samples examined were characterized by n-type conduction.
Tab. 2. Pomiary parametrów elektrycznych: koncentracji nośników n, ruchliwości μ i oporności właściwej ρ, dla próbek półprzewodnika BiTeI otrzymanych metodami VB i CVT. Temperatura pomiaru wynosiła 295 K (RT) lub 77 K. Wszystkie pomierzone próbki, posiadały przewodnictwo w typie n.

Methods	Sample number	Test temperature	n [cm^{-3}]	μ [cm^2/Vs]	ρ [Ωcm]	Conduction type
VB	BTI-1/3	295K-RT	4.70e19	2.80e2	5.53e-4	n
	BTI-1/3	77K	4.96e19	5.95e2	2.11e-4	n
	BTI-2/2	RT	3.93e19	3.04e2	5.22e-4	n
	BTI-2/2	77K	3.89E19	6.75e2	2.38e-4	n
CVT	BTI-C2/1	RT	2.65e19	1.67e2	1.41e-3	n
	BTI-C2/2	RT	2.34e19	1.96e2	1.36e-3	n

BTI-2/2 sample, was subjected to transport measurements to examine the influence of temperature (T in the range 15 - 295 K) on the following parameters: specific resistance ρ = f (T), carrier concentration n = f (T) and carrier mobility μ = f (T). The results are shown in Fig 19.

For a comparison, in Fig. 20 we show the results reported by M. Kanou and T. Sasagawa [3], concerning the in-plane resistivity vs. temperature dependence determined for the BiTeI crystals growing in the Bridgman vertical method (VB) and in the modified horizontal Bridgman HB method (Horizontal Bridgman). The BiTeI semiconductors obtained by the VB method were characterized by a concentration of n-type carriers at the level of $n \sim 6 \cdot 10^{19}$ cm^{-3}, while those obtained from the vapor phase by the VT method (Vapor Transportation) exhibited a single crystal structure and low electrical conductivity (electrical resistance greater than 1.5 MΩ at room temperature).

The above measurements show that the material obtained in ITME has the same type of conduction, i.e. n-type, and a similar resistivity at temperature 77 K ($\rho \sim 2 \cdot 10^{-4}$ Ωcm), as the material obtained by Sasagawa *et al.* and that it has a smaller carrier concentration ($n \sim 4 \cdot 10^{19}$ cm^{-3}) than that reported by the cited authors [3] ($n \sim 6 \cdot 10^{19}$ cm^{-3}).

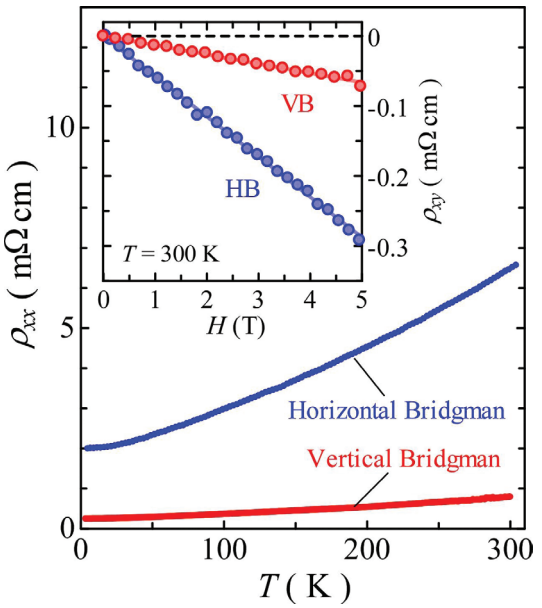

Fig. 20. Temperature dependence of in-plane resistivity (in ρ_{xx} plane) of BiTeI crystals grown by the standard vertical Bridgman (VB) method and the modified horizontal Bridgman (HB) method. Upper inset shows the dependence of Hall resistivity ρ_{xy} on magnetic field (measurements at room temperature – RT). [3]
Rys. 20. Zależność oporności właściwej (w płaszczyźnie ρ_{xx}) od temperatury, dla kryształów BiTeI wzrastających pionową metodą Bridgmana (VB) i zmodyfikowaną, poziomą metodą Bridgmana (HB). W górnej wstawce (inset), pokazano zależność oporności właściwej Halla ρ_{xy} od pola magnetycznego (H), (pomiary w temperaturze pokojowej - RT). [3]

4. Conclusions

Crystal layers of a polar semiconductor (trivial insulator) BiTeI, were obtained either by a stoichiometric synthesis and crystallization from pure elements, i.e. Te and Bi with bismuth halide BiI_3 in a quartz ampoule by the modified Bridgman method (VB) in a vertical system, or by the CVT method (chemical transport in iodine vapor) in quartz ampoules, where the previously synthesized BiTeI precursor was placed in the source zone. Iodine vapor acted as a transporting agent for the particles in a horizontal system. The wafers of dimensions 5 × 5 mm^2 were cut from the BiTeI semiconductor crystals obtained by both methods and the composition (using Raman and XRD spectroscopy), electrical properties (Van der Pauwa method) and structure (EDS) of these samples were investigated. The results confirmed the presence of a pure BiTeI phase, without precipitates, and with a uniform distribution of the constituent elements - Tab. 1.

When comparing both methods of the crystallization of the BiTeI compound, it becomes evidence that the higher the material yields the better was structural quality, obtained during a vertical crystallization using the VB method. The concentration of the majority carriers that we obtained for a BiTeI n-type semiconductor, ranging from $n \sim 2.3 \cdot 10^{19}$ to $4.9 \cdot 10^{19}$ cm^{-3}, and the resistivity at the level of $\rho \sim (5 - 17) \cdot 10^{-4}$ Ωcm, are similar to those obtained in other research centers [3, 5].

According to the reference database, the lattice parameters of BiTeI are: a = 4.3394 Å in the hexagonal plane and c = 6.8626 Å along the growth axis. XRD measurements of the layers and crystals obtained in ITME using the CVT and VB methods indicate the following values of lattice parameters: a = 4.3411 Å, c = 6.8617 Å and a = 4.3412 Å, c = 6.8587 Å, respectively. They are consistent with the data reported by other researches from various laboratories in the world, e.g to Tournier-Colletta et al. [13], where the lattice parameters for the BiTeI semiconductor amounted to: a = 4.3410 Å and c = 6.8520 Å. This data can be considered as reliable, since the deviation from the reference value is smaller than 0.5%.

A high quality BiTeCl topological insulator and a BiTeI polar semiconductor with a high theoretical value of Rashba coefficient, obtained in ITME, can be utilized for further analyses and work progress in the field of crystal growth technology of BiTeI crystals characterized by high resistance. Moreover, these materials may also open up the possibilities of a search for new quantum phenomena, such as unconventional superconductivity, spin transport and a new type of a topological non-conducting state, all arising from a unique electronic structure of these compounds. The results should also contribute to the development of a new field of physics, i.e. semiconductor spintronics.

Acknowledgements

The author would like to express their great thanks to Dr. Eng. Paweł Ciepielewski for the Raman spectroscopic measurements, to M.Sc. Magdalena Romaniec for EDS measurements, to Dr. Eng. Ryszard Diduszko for XRD analyses of the phase composition, to M.Sc. Mirosław Piersa for the measurements of electrical parameters and for M.Sc. Aleksandra Królicka for her help.

References

[1] Hsieh D., Qian D., Wray L., Xia Y., Hor Y. S., Cava R. J., Hasan M. Z.: A topological Dirac insulator in a quantum spin Hall phase, Nature, 2008, 452, 970 – 974

[2] Zhang H., Liu C. - X., Qi X. - L., Dai X., Fang Z., Zhang S. - C.: Topological insulators in Bi_2Se_3, Bi_2Te_3 and Sb_2Te_3 with a single Dirac cone on the surface, *Nat. Phys.,* 2009, 5, 438 - 442

[3] Kanou M., Sasagawa T.: Crystal growth and electronic properties of a 3D Rashba material, BiTeI, with adjusted carrier concentrations, *Journal of Physics Condensed Matter,* 2013, 25(13):135801

[4] Qi Y., Shi W., Naumov P. G., et. al., Topological quantum phase transition and superconductivity induced by pressure in the bismuth tellurohalide BiTeI, *Advanced Materials*, 2017, 29, 18, 1605965

[5] Ishizaka K., Bahramy M. S., Shin S., et al.: Giant Rashba-type spin splitting in bulk BiTeI, *Nature Materials*, 2011, 10, 7, 521 – 526

[6] Bercioux D., Lucignanoy P.: Quantum transport in Rashba spin-orbit materials: a review, *Rep. Prog. Phys*., 2015, 78, 10, 106001

[7] Sakano M., Bahramy M. S., Ishizaka K., et al.: Three--dimensional bulk band dispersion in polar BiTeI with giant Rashba-type spin splitting, *Phys. Rev. B,* 2012, 86, 085204

[8] Maaß, H., Bentmann H., Seibel Ch., et al.: Spin-texture inversion in the giant Rashba semiconductor BiTeI, *Nat. Commun.,* 2016, 7, 11621

[9] Tran M. K., Levallois J., Lerch P., et al.: Infrared- and Raman-Spectroscopy Measurements of a Transition in the Crystal Structure and a Closing of the Energy Gap of BiTeI under Pressure, *Phys. Rev. Lett.*, 2014, 112, 047402

[10] Zhou S., Long J., Huang W.: Theoretical prediction of the fundamental properties of ternary bismuth telluro-halides, *Materials Science in Semiconductor Processing*, 2014, 27, 605 – 610

[11] Van Gennep D., Linscheid A., Stewart G. R., et al.: Pressure-induced superconductivity in the giant Rashba system BiTeI, *J. Phys: Condens. Matter.*, 2017, 29

[12] Bahramy M. S., Yang B.-J., Arita R.: Emergence of non-centrosymmetric topological insulating phase in BiTeI under pressure, *Nature communications*, 2012, 3, 679

[13] Tournier-Colletta C., Autes G., Kierren B., et al.: Atomic and Electronic Structure of a Rashba p-n Junction at the BiTeI Surface, *Phys. Rev. B*, 2014, 89, 085402

[14] Babanly M. B., Tedenac J. C., Aliyev Z. S., et al.: Phase equilibriums and thermodynamic properties of the system Bi–Te–I, *J. of Alloys and Compounds*, 2009, 481, 1 – 2